



HAL
open science

On nonlinearized wavefield inversion methods and the identification of buried objects

Dominique Lesselier, Bernard Duchêne

► **To cite this version:**

Dominique Lesselier, Bernard Duchêne. On nonlinearized wavefield inversion methods and the identification of buried objects. F. Santosa and I. Stakgold. Analytical and Computational Methods in Scattering and Applied Mathematics, 1, Chapman and Hall/CRC, pp.177-194, 2000, 9781584881599. 10.1201/9780429186875-15 . hal-00637727

HAL Id: hal-00637727

<https://hal.science/hal-00637727>

Submitted on 24 Jan 2024

HAL is a multi-disciplinary open access archive for the deposit and dissemination of scientific research documents, whether they are published or not. The documents may come from teaching and research institutions in France or abroad, or from public or private research centers.

L'archive ouverte pluridisciplinaire **HAL**, est destinée au dépôt et à la diffusion de documents scientifiques de niveau recherche, publiés ou non, émanant des établissements d'enseignement et de recherche français ou étrangers, des laboratoires publics ou privés.

On Nonlinearized Wavefield Inversion Methods and the Identification of Buried Objects

Dominique Lesselier and Bernard Douchène *

Wavefield inversion is a subject that has been carefully studied by R.E. Kleinman. Some of his investigations have been carried out with the authors and their colleagues. In particular, two solution algorithms (complete family and binary-specialized modified gradient) for the retrieval of scatterers buried in a layered embedding will be examined here. But the main purpose of this contribution is to illustrate the lasting impact of his work in this demanding field both at theoretical and numerical levels, and in so doing to sketch some challenging issues to be addressed in the spirit of Kleinman's work, which is to "accelerate the transition from mathematical model to practical numerical solution" [1].

1 Introduction

The science of wavefield inversion includes nondestructive characterization of media and/or structures interrogated by a probing radiation (electromagnetic, acoustic or elastic). The signals contain encoded information about the object which is interacting with the probing wave. The inversion is but the procedure by which the signals are transformed into some intelligible form which provides us with some of this information.

A general theme of investigation comes forth (which has been considered for a number of years and with considerable success by R.E. Kleinman): the identification (including location, shape, orientation, constitutive parameters) of an object from measured scattered (or anomalous) fields which result from its interaction with known incident waves. For that purpose many solution methods

*Département de Recherche en Électromagnétisme, Laboratoire des Signaux et Systèmes, CNRS-SUPÉLEC-UPS, Plateau de Moulon, 91192 Gif-sur-Yvette Cedex, France

have been developed in the literature such as spectral methods, modified gradient and variants, complete families and equivalent sources, dual space methods, controlled level sets, stochastic techniques. In general they amount to finding a minimum of a cost functional which measures the conformity of the response of a test object to that of the original one. At best this functional reflects the fit between data and wavefield associated to the test object (observation or data equation), the satisfaction of the field equations (state or coupling equation), and the available knowledge of the user (imposition of constraints).

Two examples of nonlinearized methods in aspect-limited data configurations [12], [13], which we believe are illustrative of the complexity of an inversion machinery for ill-posed problems while exhibiting novelty and computational efficiency, are considered herein: the complete family (or distributed source) solution method, e.g., [3], [21], [5]; the binary-specialized version, e.g., [22], [9], [6], [17], [18], of the modified gradient method. (An insightful analysis of gradient-type methods is conducted in [8], whereas [11] describes a constrained modified gradient method for Maxwellian materials.)

The first method, considered in section 2, is developed in the realm of shallow water acoustics and is applied to the shape reconstruction of a sound-impenetrable cylindrical object of star-shaped, smooth cross-sectional contour which is immersed within a known, plane-layered water waveguide. One is dealing with a two-dimensional scalar case, the retrieval of the scatterer contour being carried out from range-filtered (due to waveguiding), monochromatic data using the smoothness of the sought contour as key constraint, the acoustic wavefields being modeled in the inversion from a superposition of elementary waves (the Green's functions of the waveguide).

The second method, considered in section 3, is developed in the realm of low-frequency electromagnetics (eddy currents) and is applied to the mapping of a void defect (which is identified with an unknown distribution of black voxels in an otherwise white search domain) affecting a conductive metal plate. One is now dealing with a three-dimensional vector case, the mapping of the defect being carried out from aspect-limited, frequency-diverse data using the binary aspect of the probed region as key constraint, the purely diffusive electromagnetic wavefields being modeled in the inversion from a contrast-source domain integral formulation (deduced from a dyadic Green's theorem).

In each of these two sections only one typical result of inversion is given. The analysis itself is each time mostly descriptive, mathematical derivations and numerical details being left for the referenced contributions. Notice that there purposely is no attempt to review the vast literature on each topic, but quite a large number of pertinent references are given in these contributions.

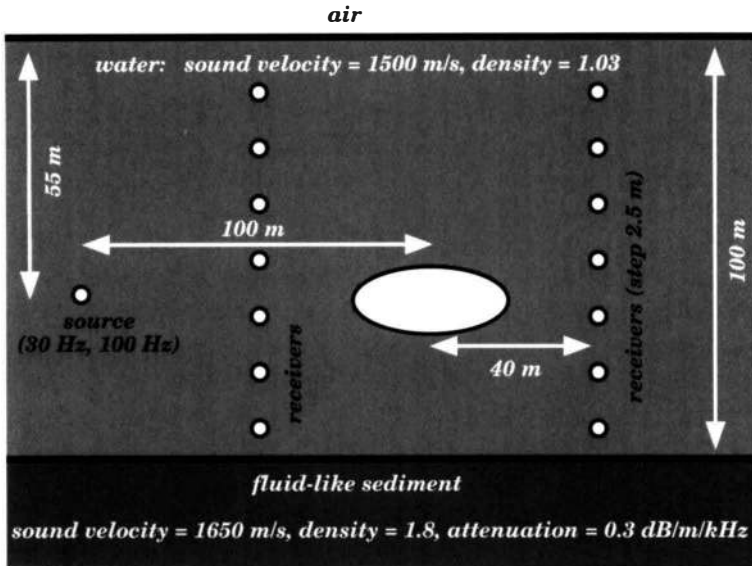


Figure 1: An impenetrable acoustical scatterer of unknown cross-sectional contour immersed in shallow water. Displayed parameters are those of a realistic (though simplified) configuration.

2 A distributed source approach in shallow water acoustics

The characterization of an obstacle immersed in shallow sea water or buried in the sea bottom from a partial observation of the pressure field which is resulting from its interaction with a given source in water is of much concern in the field of underwater acoustics, e.g., [7] and references therein.

Here (Fig. 1) we examine the prototype problem of a sound-impenetrable (hard or soft) cylindrical obstacle with star-like, smooth cross-sectional contour which is immersed in a homogeneous water column of known acoustical parameters and of finite depth. This obstacle is illuminated by at least one time-harmonic monochromatic line source also in water at some distance from it. The pressure field p typically is collected by two vertical sensor arrays which span the water column on both sides of the obstacle (long enough horizontal arrays, or other sensors arrangements, could be considered likewise). The flat sea

surface satisfies the usual pressure release condition while the boundary condition on the flat seafloor may be arbitrary; indeed, only its reflection coefficient as a function of the horizontal wavenumber plays a role in the mathematical modeling. Most of our studies were conducted for a sound-hard seafloor. We are presently investigating the case where the seafloor is modeled as a homogeneous fluid bottom half-space, though a more complicated solid elastic layering may be considered in the same way.

This nonlinear shape reconstruction in a semi- or fully-confined environment (the plate-parallel water waveguide) from data sets strongly affected by the waveguiding phenomenon, and acquired at a single frequency, is rather demanding. The analysis so far has been following two paths.

First, the unique solvability of the scattering problem has been considered from a new global radiation condition (which is an alternative to a radiation condition for each propagating mode of the waveguide), and the completeness of a family of Green's functions in the waveguide has been subsequently examined. Unique solvability is established in [4] for a sound-soft (Dirichlet) obstacle in free space or in an acoustic waveguide the walls of which satisfy Dirichlet conditions; the same was performed earlier in [3] for a Neumann condition imposed on the bottom wall, and completeness proved in this case.

However, no results have been obtained yet for the sound-hard (Neumann) obstacle; the same goes for the case of penetrable bottom (e.g., a fluid half-space). Indeed the results needed still appear out of theoretical reach. Also, it is our understanding that the demonstration of the unique solvability from the alternate radiation condition is still questioned (but how uniqueness is proved does not matter for the demonstration of the completeness). In any case certain restrictions on the obstacle contour are or should be needed (convex or at best mildly concave contour, as exhibited in the Dirichlet case) in particular in order to avoid the trapping of modes in the obstacle near field.

Second, numerical algorithms implementing the contour inversion from discrete data in various configurations have been developed. Initially the effort was directed towards sound-soft obstacles as is detailed in [21] and sound-hard ones have been considered next as is sketched in [5], with in both cases the assumption of a sound-hard seafloor. Presently, attention is on the influence of a homogeneous fluid sea bottom modeling a thick sediment layer of moderate contrast with respect to the water.

In practice one always works within an appropriate discrete setting in L_2 , and iteratively solves a penalized optimization problem whose cost functional $F = f_1 + \sigma f_2$ (σ being a penalty parameter) is a weighted sum of two residuals at the operation frequency.

The observation cost f_1 is the mean square norm of the discrepancy between the data $p^{mes}(N_R)$ collected along the measurement arrays R and the pressure $p(\Gamma, N_R)$ which would be due (at same location N_R) to a given contour Γ , normalized with respect to the data norm. It reads:

$$f_1 = \frac{\int_R |p(\Gamma, N_R) - p^{mes}(N_R)|^2 dN_R}{\int_R |p^{mes}(N_R)|^2 dN_R}. \quad (1)$$

The boundary cost f_2 is the mean square norm of the error in the satisfaction of the prescribed boundary condition along Γ (Dirichlet: the total pressure should be zero; Neumann: the normal derivative of the total pressure should be zero), the normalization being accordingly performed with respect to the norm of the incident pressure p_0 at the same location or of its normal derivative. Upon introduction of polar coordinates $\mathbf{r} = (r, \theta)$, letting $r = \gamma(\theta)$ be the radial coordinate characteristic of Γ , one has in the Dirichlet case

$$f_2 = \frac{\int_0^{2\pi} |p(\Gamma, \theta)|^2 J_\Gamma(\theta) d\theta}{\int_0^{2\pi} |p_0(\Gamma, \theta)|^2 J_\Gamma(\theta) d\theta}, \quad J_\Gamma(\theta) = \sqrt{r^2 + \left(\frac{dr}{d\theta}\right)^2}. \quad (2)$$

In the above, $p(\Gamma, \theta)$ (respectively, $p_0(\Gamma, \theta)$) is the total (respectively, incident) pressure field at point (r, θ) , $r = \gamma(\theta)$, and J is the corresponding Jacobian; the Jacobian transformation enables us not to calculate the boundary cost on the evolved contour but to do so on the fixed unit circle [2]. As for the Neumann case, it readily follows by using $\partial_n p$ instead of p .

To proceed with the optimization, Γ is described via a $2N$ sine-cosine expansion of $\gamma(\theta)$:

$$\gamma(\theta) = a_0 + \sum_{n=1}^N a_n \cos(n\theta) + \sum_{n=1}^{N-1} a_{N+n} \sin(n\theta). \quad (3)$$

The scattered pressure field $p_S = p - p_0$, considered at \mathbf{r} anywhere on, and exterior to, Γ , is equated to a weighted sum of M exact Green's functions of the waveguide $G(\mathbf{r}, \mathbf{r}_m^\Gamma)$; their source locations \mathbf{r}_m^Γ , $m = 1, \dots, M$ are located on a closed curve $\hat{\Gamma}$ which is kept inside the domain encircled by Γ and homothetic with it, via the imposition of $|\mathbf{r}_m^\Gamma(\theta)| = \alpha\gamma(\theta)$, α a constant real multiplicative factor less than 1. One has

$$p_S(\Gamma, \mathbf{r}) = \sum_{m=1}^M c_m G(\mathbf{r}, \mathbf{r}_m^\Gamma). \quad (4)$$

The complex-valued coefficients of the two finite expansions, $\{a_n\}$ and $\{c_m\}$, are determined by means of a Levenberg-Marquardt technique, usually starting from an initial circular contour inside the presumed obstacle domain and away from the sources.

For simplicity, the boundary cost f_2 is calculated by means of a trapezoidal integration rule from the discrete values of the pressure or of its normal derivative at $Q = M$ nodal points having the same regularly spaced polar angles as the M source points. Similarly, the observation cost f_1 is calculated from sums of the squared amplitudes of the field discrepancy and of the incident field at regularly spaced points of the R array(s).

Described as such, the solution method is strikingly simple. However, in the absence of a final answer yet to a number of theoretical questions, as indicated in the above, and having emphasized that the first limitation of the method is that the contour must be star-like with respect to an inner point which should be known beforehand, one is left to essentially rely on comprehensive numerical experimentation to appraise its efficiency.

Then, it is, potentially at least, applicable to many configurations once there is available an effective calculation tool of the Green's functions for source points (on the homothetic contour $\hat{\Gamma}$) and/or observation points (on the contour Γ itself) moved at each iteration in *a priori* arbitrary fashion. For the sound-hard seafloor, Green's functions are estimated by means of a hybrid ray-mode technique (refer to [21]) and for a penetrable bottom they are computed at the nodes of a regular mesh from their spectral expansion along the real wavenumber axis by appropriate fast Fourier transforms, their values at intermediate space locations being interpolated.

Nevertheless, key cases remain to be completely investigated. For example, a penetrable fluid obstacle in water will involve the critical management of sources distributed both inside the obstacle domain (to model the outer field) and outside it (to model the inner one); a solid elastic obstacle (and *a fortiori* an elastic shell) in addition to being very computer-intensive will necessarily require further theoretical examination first. The same kind of theoretical task is faced when the obstacle is partially buried in the sea bottom, whereas the case of an obstacle completely buried in a superficial layer of the sea bottom is expected to be of lesser complexity.

As for generalization to three-dimensional bodies in the water waveguide or in the bottom (with as a first step a body of revolution with axis perpendicular to the waveguide walls), which is a prerequisite to practical use, we note that the case of free space scattering configuration has been tackled with a fair success already [2].

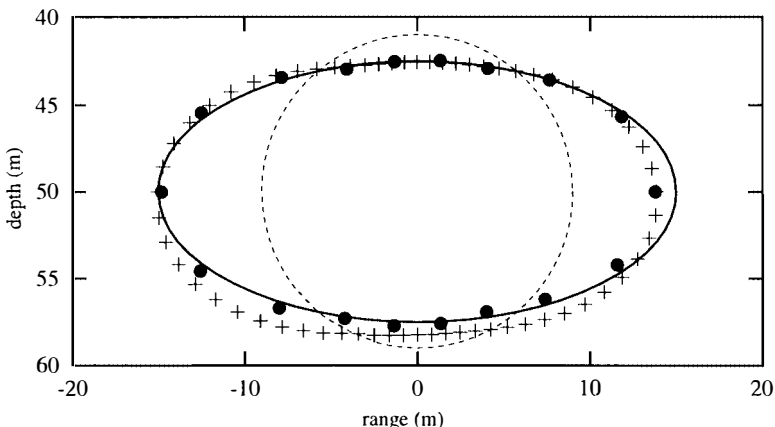


Figure 2: True (—), initial (---) and retrieved (sound-hard: +, sound-soft: •) contours of an impenetrable cylindrical elliptic obstacle (vertical and horizontal semi-axes 15 m and 7.5 m) immersed in a Pekeris-type horizontal sea channel (refer to Fig. 1). The trigonometric expansion is of order $N = 4$, the number of Green's functions and of nodal points on the contour is $M = Q = 18$ at 30 Hz and 64 at 100 Hz.

To conclude this section, we consider (Fig. 1) a sound-soft and a sound-hard elliptic obstacle in a 100 m deep acoustic channel with a sediment-like sea bottom (refer to [20]). This obstacle is illuminated from the left side (the source is at 100 m from its center) and is simultaneously viewed in the near field (at 40 m) by means of two sensor arrays, one placed on each side, so as to counterbalance the effects of the unobserved transfer of energy into the sea bottom. This is done within a frequency-hopping scheme: the obstacle is illuminated at a 30 Hz frequency first and then at a 100 Hz frequency, using the just retrieved contour as the initial contour of the new search. Notice that the wavelength in water is 50 m and 15 m, respectively, and that 4 and 13 modes are correspondingly propagated if one neglects the bottom attenuation.

The synthetic data used in the inversion, in the absence of satisfactory experimental data, have been independently calculated from a discrete version of an exact boundary integral formulation (see [21]). The contour reconstructions are displayed in Fig. 2 (courtesy of M. Lambert).

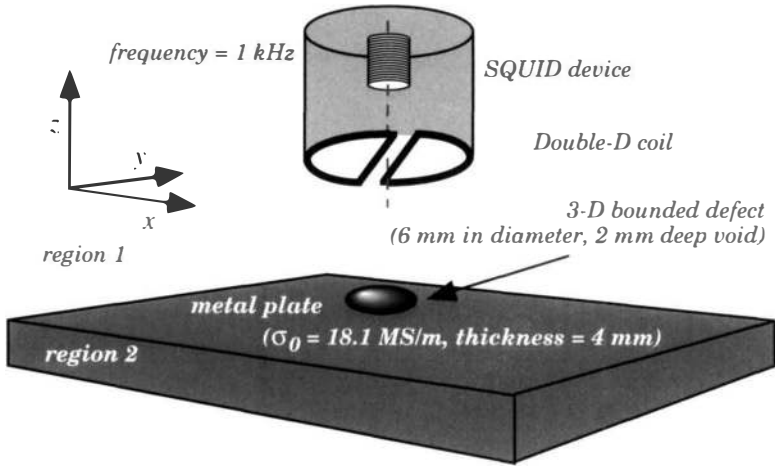


Figure 3: A metal plate probed by a double-D coil mounted below a SQUID device. Displayed parameters are typical of the experiments carried out at INFM (Napoli).

3 A binary modified gradient approach in eddy current NdE

Electromagnetic (eddy current) nondestructive evaluation of highly conductive structures is of critical concern in many applications such as in the nuclear or aircraft industry. In particular a large amount of effort is presently being devoted to the modeling of metal tubes and plates and the detection, classification, characterization and/or mapping of cracks, voids, inclusions or other damages which may affect them.

Here (Fig. 3) we examine the prototype problem of a three-dimensional bounded void defect (bulky, which is not reducible to an infinitely thin crack) found within an isotropic, nonmagnetic ($\mu = \mu_0$), horizontal metal plate of known conductivity σ_0 and illuminated by a given current source at fixed low frequency in air. We emphasize that the electromagnetic phenomenon is in practice purely diffusive.

More specifically, we are interested in inferring from a partial observation of the magnetic field in air (at best at points regularly distributed on a scanning surface parallel to the metal plate) the conductivity map of a prescribed volume D of the plate in which a defect is thought to be located, while enforcing the

hypothesis that this defect is of known constant conductivity (0 for a void defect, some other value for an inclusion of an other material). As a consequence the characteristic function of the support of the defect is the only unknown now, and the defect can be seen as a distribution of *black* voxels in an otherwise *white* domain, once a specific discretization in space has been set. No other hypotheses, such as there may be several disjoint defects, or they may not be of regular boundaries, etc. need to be assumed.

In order to do so (refer to [18]), a rigorous contrast-source vector domain integral formulation of the wavefield is developed. A standard pulse-basis, point-matching Method of Moments then yields the discrete counterparts of the formulation, whereas other variants may be used.

Several dyadic electric-electric and electric-magnetic (or vice versa) Green's functions appear in so doing. Their closed forms (refer to [18] for detailed expressions) are obtained within the two-dimensional spectral wavenumber domain, the Fourier transforms being taken with respect to the transverse (i.e., horizontal) variables, by application of a vector wave expansion method which is breaking down the dyads into independent Transverse Electric and Transverse Magnetic components.

The state equation governs the distribution of fictitious Huygens sources induced in the defect volume in the plate (region 2): at any given point \mathbf{r} , such sources $\mathbf{J}_2(\mathbf{r})$ are proportional to the total electric field $\mathbf{E}_2(\mathbf{r})$ times the contrast function $\chi(\mathbf{r}) = \sigma(\mathbf{r})/\sigma_0 - 1$, where $\sigma(\mathbf{r})$ is the conductivity at \mathbf{r} , and they obviously cancel outside the defect volume where $\sigma(\mathbf{r})$ is reduced to the embedding value σ_0 .

Assuming a time-harmonic excitation $\exp(-j\omega t)$, one has

$$\mathbf{E}_2^{inc}(\mathbf{r}) = \mathbf{E}_2(\mathbf{r}) - j\omega\mu_0 \int_D \overline{\mathbf{G}}_{22}^{ee}(\mathbf{r}, \mathbf{r}') \mathbf{J}_2(\mathbf{r}') d\mathbf{r}' \quad (5)$$

where $\overline{\mathbf{G}}_{22}^{ee}$ is the appropriate electric-electric dyadic Green's function (source and observation in region 2). As for the incident electric field $\mathbf{E}_2^{inc}(\mathbf{r})$, it is obtained by applying the dyadic Green's function $\overline{\mathbf{G}}_{21}^{ee}$ (source in the air region 1 and observation in region 2) to the current density \mathbf{J}_{source} carried by the source:

$$\mathbf{E}_2^{inc}(\mathbf{r}) = j\omega\mu_0 \int_{source} \overline{\mathbf{G}}_{21}^{ee}(\mathbf{r}, \mathbf{r}') \mathbf{J}_{source}(\mathbf{r}') d\mathbf{r}'. \quad (6)$$

The anomalous magnetic field follows by direct integration of the Huygens sources over the defect volume through the observation equation:

$$\mathbf{H}_1^{obs}(\mathbf{r}) = \mathbf{H}_1^{inc}(\mathbf{r}) + \int_D \overline{\mathbf{G}}_{12}^{me}(\mathbf{r}, \mathbf{r}') \mathbf{J}_2(\mathbf{r}') d\mathbf{r}' \quad (7)$$

where $\overline{\mathbf{G}}_{12}^{me}$ is electric-magnetic dyadic Green's function (source in region 2 and observation in region 1). As for the incident magnetic field $\mathbf{H}_1^{inc}(\mathbf{r})$, it is obtained now by applying the dyadic Green's function $\overline{\mathbf{G}}_{11}^{me}$ (source and observation in region 1) to the source current density.

We emphasize that the case of a multi-layered plate can be considered similarly, at the price of more complicated calculations of the dyadic Green's functions. A similar problem occurs in a tube (i.e., a circularly stratified cylindrical structure) which we focused upon earlier (notably from the observation of the variations of impedance of a differential air-cored probe displaced along the axis of the tube) [17].

Approximations can be devised. The quasi-static assumption leads to the cancellation of the vertical component of the Huygens sources, only their in-plane components being of importance. And from this starting point, the Localized Nonlinear approximation (LN) [17] offers both accurate results and low computational costs.

The in-plane components of the electric field inside the defect volume indeed directly result from the application of a known diagonal dyadic operator onto the in-plane components of the incident field; and the Huygens sources follow by multiplication with the contrast function:

$$\mathbf{J}_2(\mathbf{r}) = \left[\overline{\mathbf{I}} - j\omega\mu_0 \int_D \overline{\mathbf{G}}_{22}^{ee(diag)}(\mathbf{r}, \mathbf{r}') \chi(\mathbf{r}') d\mathbf{r}' \right]^{-1} \mathbf{J}_2^{inc}(\mathbf{r}) \quad (8)$$

where $\overline{\mathbf{G}}_{22}^{ee(diag)}$ consists of the diagonal components of the dyadic Green's function. Integration, led as previously, then yields the LN approximated magnetic field in air.

The inverse problem at hand can be attacked by means of modified gradient iterative schemes which retrieve both the contrast function $\chi(\mathbf{r})$ and the electric field $\mathbf{E}(\mathbf{r})$ at any \mathbf{r} in D (subscript 2 is henceforth implied) by simultaneously minimizing the residual errors in satisfying the observation equation (normalized residual f_1) and the state equation (normalized residual f_2).

Such schemes are specialized to binary objects of prescribed conductivity σ and contrast $\chi_D = \sigma/\sigma_0 - 1$ by assuming that $\chi(\mathbf{r})$ is equated to $\chi_D \Phi_\theta(\tau(\mathbf{r}))$. $\Phi_\theta(\tau)$ is a continuously differentiable function which increases monotonically between 0 and 1 when the real-valued argument τ is varied between $-\infty$ and ∞ . The smaller θ , the closer it is to a step function (or the steeper the transition between 0 and 1). A good example is $\Phi_\theta(\tau) = [1 + e^{-\tau/\theta}]^{-1}$.

In so doing, and after proper initialization, one is left with adjusting itera-

tively $\mathbf{E}(\mathbf{r})$ and the new unknown $\tau(\mathbf{r})$ along conjugate-gradient-type directions (which are calculated by maintaining either function constant), say, until the cost functional does not decrease anymore (plateau) and correspondingly, a stable gray-level map is reached. Then, decreasing θ tends to increase the contrast of this map by pushing the shade of gray of each voxel towards black or white (the shade is associated to the value of τ retrieved for this voxel via the function Φ_θ). Correspondingly, this provides us with a new initial point of the iterative scheme. This *cooling* operation can be repeated a number of times till a map which is both satisfactorily contrasted and suitably associated to a low cost functional $F = f_1 + f_2$, is reached.

The above strategy has been illustrated by several examples. The main difficulty here is mostly computational and it arises from the handling of three-component fields in a three-dimensional space, as investigated already in [17].

In view of the good performance of the LN approximation, an inversion algorithm based on this approximation has been developed from the binary-version of the modified gradient method described above. The cost functional now is reduced to a single term (the observation cost f_1) which is a nonlinear function of τ only, and which is minimized along successive conjugate-gradient directions, the binary aspect still being enforced. The iterative procedure can be sketched as follows.

Let us consider that one is able to collect only a certain number of samples of the vertical component of the magnetic field in air above the search domain D . At iteration n , the corresponding complex-valued scalar component of the residual of the vector observation equation (7) reads symbolically as

$$\rho_q^{(n)} = H_q^{obs} - \vartheta_q (\Phi_\theta^{(n)} \mathbf{E}_q^{(n)}) \quad (9)$$

where operator ϑ is defined implicitly by (7) and (8) and acts upon the two in-plane electric field components in one of Q prescribed testing configurations; each such configuration (indexed by q , $q = 1, \dots, Q$) is in effect characterized by a specific set of known electric and geometrical parameters: the operation frequency, the location of the induction probe generating the eddy currents, and the location of the magnetic field sensor. In a similar symbolic fashion, at any space point inside D one may rewrite (8) as

$$\mathbf{E}_q^{(n)} = [\bar{\mathbf{I}} - \bar{\Lambda}_q (\Phi_\theta^{(n)})]^{-1} \mathbf{E}_q^{inc}. \quad (10)$$

The normalized cost function $F = f_1$ correspondingly becomes

$$f_1 = \sum_{q=1}^Q \frac{|\rho_q^{(n)}|^2}{|H_q^{obs}|^2}. \quad (11)$$

The only unknown space function $\tau^{(n)}(\mathbf{r})$ is sought as

$$\tau^{(n)} = \tau^{(n-1)} + \beta^{(n)} \xi^{(n)} \quad (12)$$

where $\beta^{(n)}$ is position-independent. The search direction $\xi^{(n)}$ is taken of the Polak-Ribière type:

$$\xi^{(n)} = h^{(n)} + \frac{\langle h^{(n)}, h^{(n)} - h^{(n-1)} \rangle_D}{\|h^{(n-1)}\|_D^2} \xi^{(n-1)} \quad (13)$$

where $\langle \cdot, \cdot \rangle_D$ denotes the L^2 scalar product on D and $\|\cdot\|_D$ the corresponding norm. $h^{(n)}$ is the gradient of the cost functional with respect to $\tau^{(n)}$ (assuming other variables fixed) and it is expressed in closed form in terms of the adjoint operators of ϑ_q and $\bar{\Lambda}_q$. As for the displacement step $\beta^{(n)}$, it is numerically determined each time by minimizing the cost functional, a procedure which benefits from the fact that the gradient with respect to $\beta^{(n)}$ can also be written in closed form.

The whole solution procedure is started from a set of initial values $\tau^{(1)}$, for example a constant value corresponding to a contrast function of 0.5, whereas the gradient direction is chosen for the first iterate. This goes on until the cost is considered as small enough, mostly from past numerical experimentation. Cooling (the reduction of θ by a given factor) and also refreshment of the search direction into the gradient direction are performed whenever the cost stagnates as again understood from numerical experimentation.

Due to the skin effect, the shallower the defect the more it affects the data at a given operation frequency, whereas the lower this frequency the deeper the exploration depth, and as a trade-off the poorer the resolution. Though the type of source and sensor used, and the defect geometry, imply that this *rule of thumb* must be taken with caution, frequencies of the probing signals as well as the discrete spatial representation of the zone under investigation should be tailored to the expected support of the defect. This simple conclusion has been validated in the Born framework by [15]. However it remains to apply such a strategy to nonlinearized situations as underlined in [19].

Worthwhile of investigation is also the case of anisotropic layerings (such as a N -ply carbon fiber composite). Far more involved dyadic Green's functions

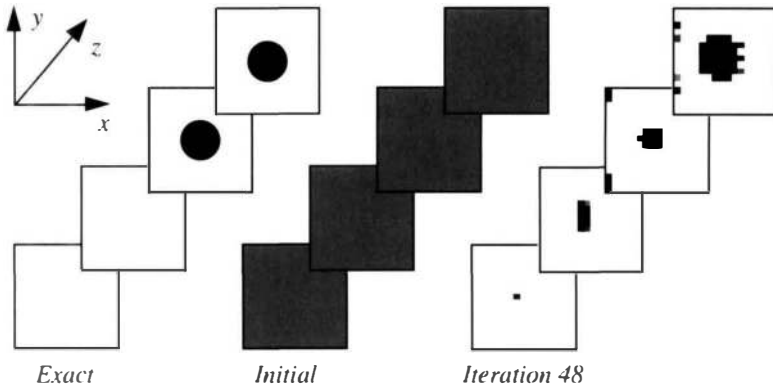


Figure 4: Gray-level cross-sectional maps of a void opening in air and machined into an aluminum plate (refer to Fig. 3 for details). These maps are retrieved within the framework of the LN approximation from a single line scan (sampling step about 1 mm) of the vertical magnetic field component observed by means of the SQUID-based measurement tool. The defect is described by 1 mm-sided cubic voxels and the search domain D comprises $16 \times 16 \times 4$ such voxels. About 60 iterations (with several cooling episodes) are needed to get to a distribution of voxels mostly black or white and fitting the data.

are needed, and independent TE and TM modes cannot be used any longer. Getting to validated and numerically stable expressions is not expected to be easy, particularly if one thinks of dealing with a large number of layers. Also, there is no immediate answer to whether or not approximations (such as the LN one) may be successfully devised in this context. The type of defect itself should also be considered carefully; bulky voids or inclusions, layer delamination, multi-branched thin cracks, and anisotropic defects due to fiber compression may each require a dedicated inversion tool.

To conclude this section, gray-level maps of a circular cylindrical void defect affecting an aluminum plate and opening in air are shown in Fig. 4 (courtesy of V. Monebhurrn).

Data (courtesy of A. Ruosi and M. Valentino) consist in discrete values of the vertical component of the magnetic field at a single frequency in air which is observed just above the center of a double-D-shaped current coil; this is a pitch-point or monostatic configuration, since coil and magnetometer are maintained at fixed elevations just above one another and displaced simultaneously.

The (newly developed) magnetometer is based on High Critical Temperature Superconductive Quantum Interference Devices (HTc SQUID), and with respect to traditional eddy current probes it has been demonstrated [23] that it offers a higher spatial resolution and greater sensitivity at very low frequencies (which enables the detection of deep subsurface defects) and at quite high liftoffs, whereas the vector domain integral formulation proved to be a suitable modeling tool of the electromagnetic interaction between the double-D coil and a number of artificial defects [18]. The inversion itself is carried out from the LN approximation.

The results of the inversion presented here are fairly good, even though the lack of information is obvious (one line scan only has been input, the measuring set-up being set to pass just above the defect mouth). Pending further investigation, this leaves hope that using data on samples from industrial origin should be fruitful.

4 Conclusion

The above analysis exemplifies that in somewhat ideal but still demanding conditions it may be possible to retrieve, with a fair accuracy, scattering objects that are at least partially unknown (in practice the constitutive material is prescribed either via a binary constraint or via a contour boundary condition) from a strongly limited observation of the results of their interaction with a known probing signal.

A key question remains [14]: is an exact description of the object required (say, in an engineering perspective)?

Indeed, one imagines how complex is the retrieval of objects in natural media (induction geophysics, shallow water acoustics, ultrasonic medical imaging, ground probing radar), or in man-made media (eddy current non-destructive evaluation, elastic characterization, microwave imaging) from experimental data which may be limited in space (vs. position of sources and/or sensors), in frequency (due to environment and/or technology), in accuracy (from unavoidable noise and other errors), or which simply may lack key elements (absence of phase due to the type of sensor, vector fields observed via one component only or through secondary quantities like a variation of impedance of a coil); and last but not least, the models on which the inversion algorithms rely are always approximated to a sometimes critical extent.

Therefore, as often emphasized by R.E. Kleinman, the algorithms must take cognizance of the shape and limitations of the data. But more modest goals

might also be aimed at, i.e., a good accomplishment may simply be the retrieval of a few distinguishing features of the sought object.

In that frame of thought, the idea of a Simplified Object (SO), which is for example prevailing in the many references on the Intersecting Canonical Body Approximation (e.g., [7]) and is sketched in [10], may be pertinent.

Three conditions however must be fulfilled simultaneously: a simple modeling of the SO behavior should be available (a handy recipe), a limited number of features should characterize the SO (clearly a lesser number of attributes than the exact one), and SO features retrieved via an inversion algorithm in accord with the recipe, should contain relevant information (a fuzzy image, certain discrepancy being accepted with the exact object).

Still, intricate nonlinearized inversion algorithms may be of good use. For example, the controlled evolution of a level set applied to the retrieval of a binary object whose contrast with respect to the environment is prescribed, and which is an alliance of the level-set description of a moving boundary and of the speed method of shape optimal design, appeared fairly immune to the lack of topological information [16].

Smoothness, single-connexity, star-shapedness, knowledge of an interior point are not imposed, only a search domain which is containing the object is required, while its extension from two-dimensional scalar cases in free space to three-dimensional vector ones in a layered embedding, may be envisaged, provided that both theoretical questions (so-called topological identification [24]) and numerical ones (parameter tuning) are addressed.

To conclude, and taking now a more personal tone, the authors would like to quote R.E. Kleinman again, from a letter he sent us in November 1997: "To analyze the past is possible, to assess the present is dangerous and to predict the future is foolhardy. Dangerous because our assessment of the current state of inverse scattering is subjective and will inevitably have unforgivable omissions thus antagonizing those omitted, and foolhardy for the obvious reason that tomorrow's advances will most probably be based on techniques not yet developed and lead in unexpected directions."

In sharp contrast with his own words, it is the belief of the authors that late Unidel Professor R.E. Kleinman was a very clever analyst of the past research, enriched by a personal experience of more than forty years, that he was fully aware of the state-of-the-art though always very kind with the solution methods of his struggling colleagues and very honest with respect to the pros and cons of his own solutions, and that he contributed to a great extent and with a lasting impact to often unexpected and always promising approaches.

Acknowledgment

Many people have contributed to the gain of expertise of the authors in the science of wavefield inversion, and have been closely involved in carrying out the research which is sketched herein. So, no attempt will be made to list them. But with regards to the development and application of the two methods specifically dealt with in sections 2 and 3, special thanks should go to (ordered per geographical distance) M. Lambert, V. Monebhurrun, and C. Rozier (LSS, Gif-sur-Yvette), A. Ruosi (INFM, Naples), and T.S. Angell (CMW, Newark); S. Riggs also deserves recognition for her contribution to several of the first author's presentations, in addition to her role in his lasting relationship with R.E. Kleinman. Acknowledgments of financial support should correspondingly go to CNRS, EDF, INFM, NSF, and NATO.

References

- [1] T.S. Angell, Mathematical and numerical methods for analysis and design of electromagnetic fields, *Interim Report*, Multidisciplinary University Research Initiative Project, Air Force Office of Scientific Research, Grant F49620-96-1-0039, May 1998, <http://www.udel.edu>.
- [2] T.S. Angell, J. Jiang, and R.E. Kleinman, A distributed source method for inverse acoustic scattering, *Inverse Problems*, **13**(1997), 531-546.
- [3] T.S. Angell, R.E. Kleinman, C. Rozier, and D. Lesselier, Uniqueness and complete families for an acoustic waveguide problem, Center for the Mathematics of Waves, Technical Report 96-4, University of Delaware, Newark, 1996.
- [4] T.S. Angell and R.E. Kleinman, Radiation condition and uniqueness, Center for the Mathematics of Waves, Technical Report 97-2, University of Delaware, Newark, 1997.
- [5] M. Bocly, M. Lambert, C. Rozier, and D. Lesselier, Optimal contour reconstruction of a sound-hard obstacle in a shallow water acoustic waveguide, in *Underwater Acoustics*, A. Alippi and G.B. Canelli, eds., CNR-IDAC, Rome, 1998, 643-648.
- [6] B. Duchêne, D. Lesselier, and R.E. Kleinman, Inversion of the 1996 Ipswich data using binary specializations of modified gradient methods, *Antennas and Propagation Magazine*, **39**(1997), 9-12.

- [7] R.P. Gilbert, T. Scotti, A. Wirgin, and Y. Xu, The unidentified object problem in a shallow ocean, *Journal of the Acoustical Society of America*, **103**(1998), 1320-1328.
- [8] R.E. Kleinman and P.M. van den Berg, Gradient methods in inverse acoustic and electromagnetic scattering, in *Large Scale Optimization*, L.T. Biegler, T. Coleman, A. Conn, and F. Santosa, eds., Springer, Berlin, 1997, 173-194.
- [9] R.E. Kleinman, P.M. van den Berg, B. Duchêne, and D. Lesselier, Location and reconstruction of objects using a modified gradient approach, in *Inverse Problems of Wave Propagation and Diffraction*, G. Chavent and P.C. Sabatier, eds., Springer, Berlin, 1997, 143-158.
- [10] R.E. Kleinman, D. Lesselier, and A. Wirgin, On the retrieval of simplified objects in wavefield inversion, in *Proceedings 1998 Progress in Electromagnetics Research Symposium* (Nantes), 1998, 174-178.
- [11] M. Lambert, D. Lesselier, and B. Kooij, The retrieval of a buried cylindrical obstacle by a constrained modified gradient method in the H-polarization case and for Maxwellian materials, *Inverse Problems*, **14**(1998), 1265-1283.
- [12] D. Lesselier and B. Duchêne, Wavefield inversion of objects in stratified environments. From backpropagation schemes to full solutions, in *Review of Radio Science 1993-1996*, W.R. Stone, ed., Oxford University Press, Oxford, 1996, 235-268.
- [13] D. Lesselier and B. Duchêne, The inversion of objects buried in a layered embedding: the outline of a multi-pronged investigation, in *First EMSL User Workshop Proceedings*, G. Nesti et al. eds., EUR Report 17326 EN, Brussels, 1997, 67-74.
- [14] D. Lesselier and A. Wirgin, Identification d'objets ou milieux par inversion de signaux acoustiques ou électromagnétiques, in *Problèmes Inverses*, M. Bonnet, ed., "Arago", Lavoisier, Paris, 1999.
- [15] A. Litman and D. Lesselier, On attenuation-matched inversion methods of diffusive wavefields, *Inverse Problems*, **15**(1999), 1-13.
- [16] A. Litman, D. Lesselier, and F. Santosa, Reconstruction of a 2-D binary obstacle by controlled evolution of a level set, *Inverse Problems*, **14**(1998), 685-706.

- [17] V. Monebhurrun, B. Duchêne, and D. Lesselier, 3-D inversion of eddy current data for nondestructive evaluation of steam generator tubes, *Inverse Problems*, **14**(1998), 707-724.
- [18] V. Monebhurrun, D. Lesselier, B. Duchêne, A. Ruosi, M. Valentino, G. Pepe, and G. Peluso, Eddy current nondestructive evaluation using SQUIDS, in *Electromagnetic Non-Destructive Evaluation (III)*, D. Lesselier and A. Razek, eds., IOS Press, Amsterdam, 1999, 171-181.
- [19] V. Monebhurrun, A. Litman, D. Lesselier, and B. Duchêne, Inversion of binary objects at eddy current frequencies in a wavefield framework. Application to the nondestructive evaluation of conductive plates and tubes, in *Proceedings 1998 URSI International Symposium on Electromagnetic Theory*, Thessaloniki, 1998, 766-768.
- [20] C. Rozier and D. Lesselier, Inversion of a cylindrical vibrating body in shallow water from aspect-limited data using filtered SVD and the L-curve, *Acta Acustica*, **82**(1996), 717-728.
- [21] C. Rozier, D. Lesselier, T.S. Angell, and R.E. Kleinman, Shape retrieval of a cylindrical obstacle immersed in shallow water from single-frequency farfields using a complete family method, *Inverse Problems*, **13**(1997), 487-508.
- [22] L. Souriau, B. Duchêne, D. Lesselier, and R.E. Kleinman, A modified gradient approach to inverse scattering for binary objects in stratified media, *Inverse Problems*, **12**(1996), 463-481.
- [23] M. Valentino, A. Ruosi, G. Pepe, and G. Peluso, Superconductive and traditional electromagnetic probes in eddy current NDE for detection of deep defects, in *Electromagnetic Non-Destructive Evaluation (III)*, D. Lesselier and A. Razek, eds., IOS Press, Amsterdam, 1999, 159-170.
- [24] J.-P. Zolésio, A. Litman, and D. Lesselier, Topological identification in electromagnetic wavefield inversion, in *Proceedings 1998 International Symposium on Boundary Elements Methods*, Palaiseau, 1998, 209-210.